

**METAL-CENTRIC PERSPECTIVE OF A LAYERED CHONDRULE IN THE CR CHONDRITE ACFER 139: INSIGHTS FROM ELECTRON BACKSCATTERED DIFFRACTION.** E. J. Crapster-Pregont<sup>1,2</sup>, W. H. Towbin<sup>3</sup>, and D. S. Ebel<sup>1,2</sup>. <sup>1</sup>Lamont-Doherty Earth Observatory, Columbia University, Palisades, NY, 10964, USA ([ellencp@ldeo.columbia.edu](mailto:ellencp@ldeo.columbia.edu)). <sup>2</sup>Dept. of Earth and Planetary Science, American Museum of Natural History, New York, NY, 10024, USA ([debel@amnh.org](mailto:debel@amnh.org)). <sup>3</sup>Microscopy and Imaging Facility, American Museum of Natural History, New York, NY, 10024, USA ([htowbin@amnh.org](mailto:htowbin@amnh.org)).

**Introduction:** Chondrites and their components are the keys to understanding the chemical and dynamic history of our early solar system. Carbonaceous Renazzo-type (CR) chondrites have experienced low amounts of aqueous parent body alteration and minimal thermal alteration [1]. CR chondrites also contain high modal abundances of chondrules making them ideal for testing chondrule formation hypotheses [2]. Acfer 139 (CR2) is a minimally altered Saharan find. Many different types of chondrules are present and most exhibit metal layers or rims. Among the different types of chondrules, layered chondrules remain most enigmatic, especially those with multiple layers of metal.

Several studies have explored metal layers in CR chondrules [e.g. 3-13]. This metal-centric study examines the chemical and textural relationships between the metal layers and the surrounding silicate layers in a complex layered chondrule in Acfer 139. This chondrule was previously described by [14] and a parallel silicate-centric study of its inner layers is reported by [15].

**Method:** Serial thick section AMNH 4793-t2-ps5B [cf. 15] of Acfer 139 was embedded in a 1-inch epoxy round. The sample was polished to obtain an EBSD quality surface with the following protocol: SiC paper 400 grit 20s, 600 grit 20s, 800 grit 20s, 1200 grit 40s (2x 20s); diamond slurry 5  $\mu\text{m}$  15min, 3  $\mu\text{m}$  10min, 1  $\mu\text{m}$  20min; 0.3  $\mu\text{m}$   $\alpha$ -alumina slurry 15min; 0.05  $\mu\text{m}$  colloidal silica 30min. All this was done by hand except the colloidal silica which was done using a Buehler Mini-Met. A Buehler Tex-Met polishing pad was used with all slurries. No carbon coat was applied to the repolished sample, 4793-t2-ps5B2.

An EDAX DigiView IV electron backscatter diffractometer attached to a Zeiss variable-pressure EVO 60 scanning electron microscope was used for orientation analysis. EDAX OIM software was used to create orientation maps and conduct point analyses while EDAX TEAM software was used to obtain elemental information with an EDAX energy dispersive spectrometer (EDS).

**Results:** The polishing technique successfully prepared both metal and silicate grains within the sample (Fig. 1; cf. [15]). Secondary electron (SE) images

of the metal show minimal shadowing which would be due to topographic variation. Variation in grayscale within the metal is due to chemical and/or orientation variation.

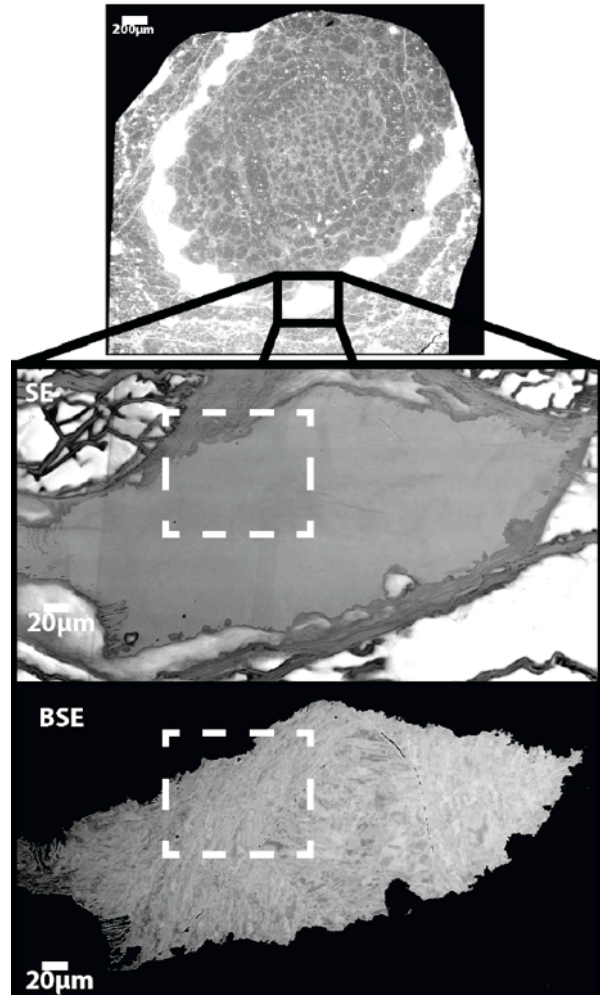


**Figure 1:** BSE of layered chondrule (top) in Acfer 139. SE (middle) and BSE (bottom; exaggerated contrast) of a metal nodule in the second metal layer. SE image shows minimal surface topography. Dashed box is area shown in Fig. 2b.

Two metal nodules in the second metal layer were mapped at varying resolutions and false-color maps were generated. The false color assigned to each pixel corresponds to the reverse pole figure as defined in the key in Fig. 2. Each nodule appears to have at least two regions of distinct orientations indicating different

grains. There are sub-parallel lamellar-like features transecting the nodules.

**Discussion:** So far in this study, only a few nodules of metal have been analyzed in the second concentric metal layer [15] of the Acfer 139 layered chondrule [14]. The application of EBSD mapping to the nodules shows that each is actually several grains, observed as different regions of uniform orientation (Fig. 2a). The lamellar-like features share similar orientations (Fig. 2a and b). These features are not an artifact of the polishing protocol (Fig. 1). Possible explanations for these features include exsolution of more Ni-rich kamacite, twinning of kamacite, or Neumann lines.

More detailed chemical analysis is needed to determine if there is chemical variation associated with these features. Chemical mapping in the SEM and EPMA do not indicate significant chemical variation within nodules, but would not capture submicron variation. Pressure-induced Neumann lines have been documented in kamacite [16]. Such a feature would help constrain the physical history of this layered chondrule based on its presence or absence in each metal layer. None of these three possibilities can be ruled out at this point.

**Future Work:** Many hypotheses regarding metal layer formation in chondrules have been proposed [7-13]. None of these studies have looked in detail at the orientation of the metal grains and their relationship to their surrounding silicates.

Here, we focus on the larger, platy metal grains of the second metal layer in the Acfer 139 chondrule. More information could be extracted, particularly from the inner layer of 1-5  $\mu\text{m}$  spherical grains. Similar

orientation analysis will be conducted for multiple grains in each of the three distinct metal layers in the Acfer 139 layered chondrule [14]. Understanding the similarities and differences between each of these metal layers is essential to determining the dynamic conditions during the sequential formation of igneous layers in this chondrule and in chondrules exhibiting similar characteristics.

**Acknowledgements:** This research is supported by NASA Cosmochemistry grant NNX10AI42G (DSE) and the National Science Foundation Graduate Research Fellowship Program (DGE-11-44155) (ECP).

**References:** [1] Weisberg M. K. et al. (2006) *Meteorites and the Early Solar System II*, Univ. Arizona Press, 19-52. [2] Bayron J. M. et al. (2014) *LPS XLV*, Abstract #1225. [3] Kong P. et al. (1999) *GCA*, 63, 2637-2652. [4] Lee M. S. et al. (1992) *GCA*, 56, 2521-2533. [5] Humayun M. et al. (2002) *LPS XXXIII*, Abstract #1965. [6] Humayun M. et al. (2010) *LPS XLIV*, Abstract #1840. [7] Zanda B. et al. (2002) *GCA*, 66, A869. [8] Kong P. and Palme H. (1999) *GCA*, 63, 3673-3682. [9] Conolly H. C. et al. (2001) *GCA*, 65, 4567-4588. [10] Weisberg M. K. et al. (2002) *Meteoritics & Planet. Sci.*, 37, A149. [11] Campbell A. J. et al. (2005) *Chondrites and the Protoplanetary Disk*, 341, 407-431. [12] Ebel D. S. et al. (2008) *Meteoritics & Planet. Sci.*, 43, 1725-1740. [13] Wasson J. T. and Rubin A. E. (2010) *GCA*, 74, 2212-2230. [14] Ebel D. S. and Downen M. R. (2011) *Meteoritics Planet. Sci. Suppl.*, 46, A62. [15] Hobart K. K. et al. (2015) *LPS XLVI*, Abstract #1978. [16] Ramdohr P. (1973) *The Opaque Minerals in Stony Meteorites*, Elsevier, 245p.

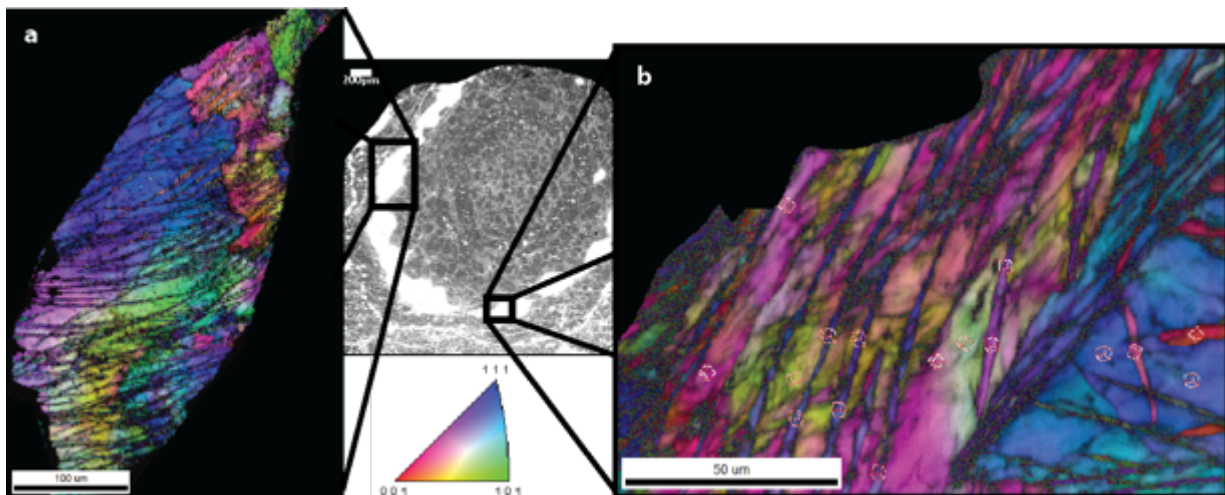


**Figure 2:** EBSD generated false color, reverse pole figures maps for a whole metal nodule (a; 2  $\mu\text{m}/\text{pixel}$ ) and outlined area of nodule from Fig. 1 (b; 0.5  $\mu\text{m}/\text{pixel}$ ) in the second metal layer in the Acfer 139 layered chondrule. Color represents the orientation of the metal at each pixel described by the mixing chart in the center of the figure. Small wire-frame cubes highlight the orientation of various regions. Lamellar-like features are not artifacts of the polishing process, see Fig. 1.